

## Ambient seismic noise levels: a survey of the permanent and temporary seismographic networks in Morocco

### *Bruit de fond sismique: interpellation des réseaux sismographiques permanents et temporaires au Maroc*

Younes EL FELLAH<sup>\*1,2</sup>, Abd El-Aziz KHAIRY ABD EL-AAL<sup>3</sup>, Lahcen EL MOUDNIB<sup>1,2</sup>, Mimoun HARNAFI<sup>1</sup>, Driss EL OUAI<sup>1</sup>, Mohamed Majid HIMMI<sup>2</sup>, Mimoun CHOURAK<sup>4</sup>, Antonio VILLASEÑOR<sup>5</sup>, Josep GALLART<sup>5</sup> & Christine THOMAS<sup>6</sup>

1. Earth Sciences Department, Scientific Institute, Mohammed V University of Rabat, Morocco. \* (Email: el.fellah.younes@gmail.com).

2. Applied Physics Department, Faculty of Science, Mohammed V University of Morocco.

3. Seismology Department, National Research Institute of Astronomy and Geophysics, Helwan, Cairo, Egypt.

4. Earth Sciences Department, Pluridisciplinary Faculty, University Mohammed I, Nador, Morocco.

5. Earth Sciences Department, Jaume Almera Institute, CSIC, Barcelona, Spain.

6. Geophysics Department, Institut für Geophysik, University of Münster, Munster, Germany.

---

**Abstract.** We present, in this paper, the results of an analysis of the variations in ambient seismic noise levels from data collected for the first time in Morocco. For this purpose, 23 broadband seismic stations were deployed in different structural domains covering Rif Mountains, Middle and High Atlas and parts of the Anti-Atlas. We calculated power spectral densities (PSD) of background noise for each ground motion component recorded at different sites, and then compared the results with the high-noise and low-noise models of Peterson (1993). Time intervals (of day and night) were indiscriminately considered for computation of noise level regardless of the selected earthquakes. Furthermore, we have extended the discussion about noise to different frequency bands of interest. We found several variabilities in the PSD levels at all stations. The significant variability was observed at long periods in most stations. The results of this study could be used to evaluate future emplacements of new seismic stations and therefore can help to develop new seismic noise models in North Africa.

**Keywords :** Ambient seismic noise, power spectral density, Peterson models, seismic arrays, Morocco.

**Résumé.** Nous présentons, dans cet article, quelques résultats issus de l'étude du bruit de fond collecté pour la première fois à partir des réseaux sismiques Broadband installés au Maroc. A cet effet, 23 stations sismiques ont été déployées dans différents domaines structuraux couvrant les chaînes du Rif, Moyen et Haut Atlas et des parties de l'Anti-Atlas. Nous avons calculé la densité spectrale de puissance (DSP) du bruit de fond pour chaque composante du mouvement du sol enregistrée à différents sites, puis nous avons comparé les résultats avec les limites supérieures et inférieures du modèle de Peterson (1993). Toutes les tranches temporelles (jour comme nuit) ont été investies sans considération des tremblements de terre. Les résultats de cette étude pourraient être utilisés pour évaluer l'emplacement de nouvelles stations sismiques et développer de nouveaux modèles de bruit sismiques en Afrique du Nord.

**Mots-clés :** Bruit de fond sismique, densité spectrale de puissance, modèle de Peterson, réseaux sismiques, Maroc.

---

## INTRODUCTION

Variations in the noise level may have a significant effect on the detection capability of a seismic network (Sheen et al. 2009, D'Alessandro et al. 2013). The usefulness of seismic data increases greatly when noise levels are reduced. A good quantification and understanding of the seismic noise is a first step for seismic noise reduction purposes (McNamara & Buland 2004, D'Alessandro et al. 2013). Baseline noise models have been commonly used for the configuration of a seismic station network (Peterson 1993, McNamara & Buland 2004, Berger et al. 2004, Sleeman et al. 2006, Bahavar & North 2002). In this study we have analyzed the background seismic noise level in several zones of Morocco. Diaz et al. (2009) and D'Alessandro et al. (2013) have carried similar works in the neighborhood area of Iberia. The main sources of seismic noise are natural or ambient disturbances such as

wind, sea waves, traffics, industrial machinery, etc. Several studies indicate that the principal natural noise sources include microseisms, diurnal temperature and other atmospheric parameters (Zürn & Widmer 1995, Beauduin et al. 1996), flow and waves associated to regional rivers and lakes. Principal anthropic sources of noise (high frequencies above 0.3 Hz) come generally from transportation infrastructure as roads, highways, railways, pipelines, etc (e.g., Rodgers et al. 1987, Given 1990, Gurrola et al. 1990, Given & Fels 1993, Peterson 1993, Withers et al. 1996, Young et al. 1996, Vila 1998, Uhrhammer 2000). Wind is the predominant high-frequency noise source at remote sites (e.g., Withers et al. 1996). Some additional information about noise composition can be obtained from the results of Webb (1998), Zhang et al. (2009) and Chouet et al. (1998); the latter have analyzed the volcanic tremor and found a very significant

proportion of surface waves in the total noise power. Other recent works on ambient seismic noise sources, noise types and noise spectral analysis can be found in Abd el-aal (2010a, b, c) Abd el-aal (2011), Abd el-aal (2012), Abd el-aal & Soliman (2013), Zhang *et al.* (2012), D'Alessandro *et al.* (2013), Stankiewicz *et al.* (2012) and Badal *et al.* (2013).

We have conducted this study with the following aims:

To gather a set of ambient seismic noise spectra for broadband stations belonging to recently deployed seismographic networks in Morocco;

To assess the effects of the temporary seismic vault construction;

To determine the time needed for noise sites stabiliza-

tion; to establish characteristics and origin of the seismic noise at those sites;

To evaluate the suitability of the current station locations and future places for installation of permanent stations.

## TECTONIC SETTING

The study area covers a parts of the central and northern parts of Morocco (Fig. 1). This region is characterized by the complexity of the seismotectonic pattern, despite of its moderate seismic activity associated to the convergence between Africa and Eurasia tectonic plates (Galindo-Zaldívar *et al.* 1999, Negredo *et al.* 2002, López\_Casado *et al.* 2014), Tahayt *et al.* 2008, Medina *et al.* 1988).

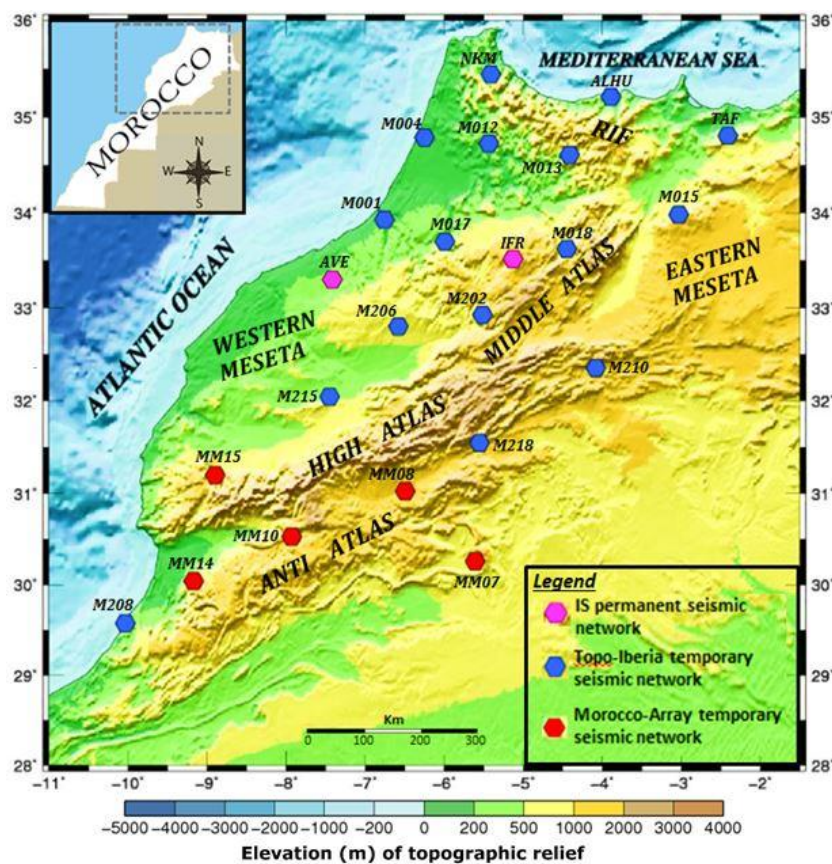


**Figure 1.** Topographic map showing the temporary and permanent broadband stations deployed in northern Morocco, adapted with Generic Mapping Tools (GMT) Wessel and Smith (1991). The elevations (m) of the topographic relief are indicated on the color scale.

In this area, different structural domains can be distinguished from north to south: Rif Mountains, Middle and High Atlas, Moroccan Meseta and Anti Atlas (Fig. 2). Rif Mountains and the Betic Cordilleras constitute the Westernmost end of the Alpine orogenic belt. This orocline results from the Cretaceous to Paleogene collision of the Eurasian and African plates. Structural contacts between thrust sheets and nappes generally dip to the South in the Betics and to the North in the Rif; that is, toward a central “internal zone”. The internal zone of the Betic-Rif orogen is common to both Cordilleras and consists of metamorphic

complexes, showing N-S continuity below the Alboran Sea; these units define the so-called Alboran domain. Mountain ranges in the internal zone are separated by “flysch zone” (Neogene intramontane basins), they consist of nappes which include deep-water sediments (radiolarites, turbidites) and some ophiolitic slivers are thought to be detached from a Mesozoic ocean–or transitional crust–floored through the North of the African margin.

The Gibraltar Arc is thought to be a result of westward overthrusting of the Alboran domain onto Iberian and Maghrebian crust. (Sanz de Galdeano 1990).

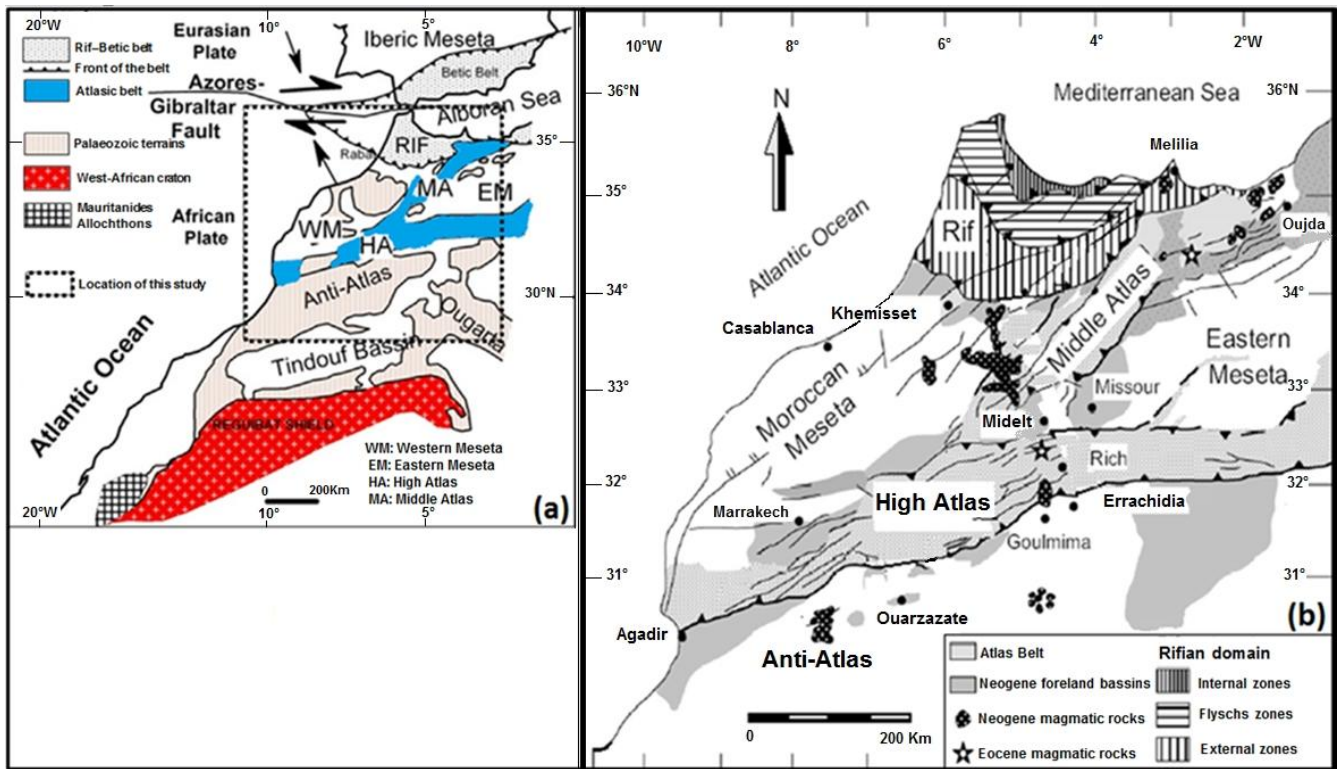


Figure 2. a. Tectonic units in Morocco; b. The main geological formations in the study area (Piqué and Michard, 1989, modified)

The Moroccan Meseta (Fig. 2) shows the effect of Variscan orogeny (Piqué & Michard 1989). This Variscan belt is divided into the Western and Eastern Meseta, separated by the Mesozoic rocks of the Middle Atlas. The Central Massif exhibits a complete Palaeozoic sequence. The Eastern Meseta can be distinguished from the Western Meseta in two main respects. First, it records different sedimentary environments, the Silurian being represented in the Eastern Meseta by pelagic deposits and the early–middle Devonian by turbidites. Second, both the intensity (greater in the Eastern Meseta) and the age of the first deformational event (Late Devonian in the Eastern Meseta and Carboniferous in the Western Meseta) are different. As a whole, the Eastern Meseta can be interpreted as recording some crustal thinning, which gave way to an open sea to a pelagic sedimentary realm during the upper part of the Early Palaeozoic.

The Anti-Atlas is a marginal up doming of the Precambrian of the West African Craton, which acted as a stable crust during the Alpine orogeny. The Atlas Mountains were developed from Mesozoic rift grabens. These rifts were reversed since the Cenozoic, and form the present-day Atlas range as a peri-Mediterranean Alpine system (Beauchamp *et al.* 1999). These mountains are separated by two rigid and stable Palaeozoic blocks, namely the Western and Eastern Meseta. To the South, the High Atlas is separated from the West African Craton (Anti-Atlas) by the so-called “South Atlasic Fault” (SAF) or “South Atlas Front” (Frizon de Lamotte *et al.* 2000). The Anti Atlas exposes Precambrian

through Palaeozoic rocks of the West African Craton. The Late Proterozoic rocks were affected by the Pan-African orogeny and by a deformation of the Hercynian. In the Late Palaeozoic, the dislocation of the Pangean plate by a post-convergent extension caused the development of extensive episodes, recorded in the Late Triassic–Early Jurassic synrift basins, that were initiated by the reactivation of older Hercynian–Alleghanian thrusts (Laville *et al.* 2004).

### FIELDWORK AND STATIONS

This section is devoted to the description of the conditions that were considered during the installation. Temporary field installations (Tab. 1) for short period observations may put other demands on seismometer installation than permanent installations for broadband observations.

#### Fieldwork

For sensitive short period observations we have primarily sought sites without local vibrational sources. High-resolution broadband observations on the other hand require careful thermal shielding and protection against air-pressure variations, since forces due to these unwanted sensitivities do not decrease as rapidly with increasing signal-period as the inertial forces do due to ground motion. In general, when a suitable place has been found (roughly level and large enough for the sensor and the insulating box), the loose surface material is removed using a back hoe and/or a shovel and the

exposed rock is cleaned off using a geologic hammer and a wire brush in order to get a clean and stable surface. The two permanent installations that belong to the Scientific Institute (AVE and IFR) are placed in a seismometer vault. As for temporary site stations (Fig. 3), the vault is designed by four panes: location; protection; coupling and shielding. We dug a hole of about 70 cm, we put concrete above which, we placed above a vault of 70 cm height and 40 cm diameter. In this container, we put about 10 cm thick of dry sand. We laid a tile on the sand, adjusted it to the horizontal plan and then we put above it the seismometer, with respect to North direction. The container was then completely covered. This installation method provides good insulation against wind and sudden rise in temperature. The sand, placed at the bottom of the container, reduces the high frequency vibrations.

Typically, additional potential sites in an area are investigated in order to find a new site for a broadband station, for which noise tests are done at pre-selected spots. The optimal places for these stations should be located on public lands with nearby power and telephone and away from significant sources of cultural noise (roads, highways, railroads, etc.). Positions with minimal exposure to direct sunlight are also preferred for thermal stability. Considerations against human and animal disturbance were taken into account. For these stations, we preferred locations that offer some degree of security and are not generally visible for the public. Thermal insulation has perhaps the largest impact on the overall performance of the seismometer and it has an advantage of being both inexpensive and easy to install. The objective is to achieve a constant temperature, as

long as possible, to significantly attenuate the diurnal thermal signature. Temperature changes with time; particularly, diurnal changes which are much more important than the high or low average temperature. Many broadband seismometers require mass centering, if the temperature "slips" more than a few degrees Celsius, although their operating range is much wider. Furthermore, temperature changes can cause problems with mechanical and electronic drifts, which may seriously deteriorate the quality of seismic data at very low frequencies (Uhrhammer *et al.* 1998). In general, thermal drifts should be kept acceptably small by thermal insulation of the vault. Maximum  $\pm 5^{\circ}\text{C}$  short-term temperature changes can be considered a target for passive short-period seismometers and force-feedback active accelerometers. To fully exploit the low-frequency characteristics of a typical 30 second period broadband seismometer, the temperature must be kept constant within less than  $1^{\circ}\text{C}$ . In summary, all the above-mentioned criteria were taken into consideration when deploying each station.

### Stations

We used 23 Broadband stations covering central and northern parts of Morocco. These stations were equally distributed on the field (Fig. 2). Two permanent stations of the Scientific Institute were installed in Averroes (AVE) and Ifrane (IFR) observatories; Sixteen ICJTA temporary broadband stations were implemented in different region within the Topo-Iberia project, covering northern and central parts of the country and Five IFG temporary broadband stations were deployed in the South of the study area.

**Table 1.** Stations parameters.

Stations	Number of components	Sensor type	Digitizer type	Communication	Latitude(°)	Longitude(°)	Altitude (meter)	Length of data (in days)	Data Year used	Institution
AVE	3	STS-2	Quanterra Q330	Satellite	33.298100	-7.413300	230.0	170	2009	IS*
IFR	3	STS-2	Quanterra Q330	Internet	33.5166	-5.1272	1630.0	150	2009	IS
ALHU	3	Trillium 120	Taurus	Flash disk	35.213270	-3.890140	63.0	200	2009	ICJTA*
M001	3	Trillium 120	Taurus	Flash disk	33.929260	-6.756040	192.0	130	2010	ICJTA
NKM	3	Trillium 120	Taurus	Flash disk	35.447600	-5.410420	423.0	180	2010	ICJTA
M004	3	Trillium 120	Taurus	Flash disk	34.791830	-6.249770	119.0	70	2010	ICJTA
TAF	3	Trillium 120	Taurus	Flash disk	34.810040	-2.411610	854.0	365	2011	ICJTA
M012	3	Trillium 120	Taurus	Flash disk	34.730060	-5.434270	227.0	265	2009	ICJTA
M013	3	Trillium 120	Taurus	Flash disk	34.610330	-4.414590	537.0	300	2009	ICJTA
M015	3	Trillium 120	Taurus	Flash disk	33.984530	-3.035030	1079.0	150	2010	ICJTA
M017	3	Trillium 120	Taurus	Flash disk	33.698810	-5.990600	657.0	160	2011	ICJTA
M018	3	Trillium 120	Taurus	Flash disk	33.622850	-4.448540	1090.0	310	2011	ICJTA
M202	3	Trillium 120	Taurus	Flash disk	32.922180	-5.513684	1443.5	365	2011	ICJTA
M206	3	Trillium 120	Taurus	Flash disk	32.801315	-6.578210	748.9	350	2011	ICJTA
M208	3	Trillium 120	Taurus	Flash disk	29.578123	-10.032167	114.5	355	2011	ICJTA
M210	3	Trillium 120	Taurus	Flash disk	32.354267	-4.082016	1432.7	355	2011	ICJTA
M215	3	Trillium 120	Taurus	Flash disk	32.046501	-7.449135	518.8	355	2011	ICJTA
M218	3	Trillium 120	Taurus	Flash disk	31.547239	-5.551305	1403.0	360	2011	ICJTA
MM07	3	Trillium 120	Taurus	Flash disk	30.258400	-5.608400	731.0	365	2011	IFG*
MM08	3	Trillium 120	Taurus	Flash disk	31.025900	-6.492100	1278.0	365	2011	IFG
MM10	3	Trillium 120	Taurus	Flash disk	30.529900	-7.928400	1058.0	365	2011	IFG
MM14	3	Trillium 120	Taurus	Flash disk	30.042400	-9.169400	774.0	365	2011	IFG
MM15	3	Trillium 120	Taurus	Flash disk	31.199100	-8.897300	955.0	365	2011	IFG

\*IS : Institut Scientifique ; ICTJA : Institut de Ciencias de la Tierra Jaume Aimeria ; IFG : Institut für Geophysik



Figure 3. Instruments, materials and installations involved in the emplacement of permanent and temporary broadband stations. a. Temporary installation of a broadband seismometer at a potential site. b. Buried sensor covered with an insulating box to provide thermal stability; the data logger and the batteries are in the black box. c. Some kind of synthetic wool, polyester stuffing or fleece material, which is wrapped around the seismometer. d. Plastic tube where the sensor is buried below the surface. e. Vault containing the seismometer, which is usual in this type of installations. f. The transmissions room that contains the transmitter, digitizer and other materials. g. AVE sensor. h. The satellite dish, used to send the information to the main data centers.

All the equipment of temporary stations are homogeneous, seismometers are Nanometrics Trillium 120P type, with Taurus dataloggers, which continuously record data sampled at a rate of 100 samples/sec.

However, for the permanent stations, the seismometers are STS2 type with Quanterra Q330 dataloggers, which also saves data continuously at the same rate (Tab. 1). We calculated power spectral densities of background noise for each component of each broadband seismometer, deployed in different sites; then we compared them with the high and low-noise Model of Peterson (1993). All segments from day and night local time windows were included in the calculation, without parsing out earthquakes. Calculations performed in this study were based on Fortran and Matlab codes, developed and applied at each station. These codes process, analyze and compare the obtained results with the Peterson Model.

### POWER SPECTRAL DENSITY CURVES

The power spectral densities (PSDs) of background noise were performed for each component of each deployed broadband seismometer. We focused on the noise spectra within three frequency intervals: long period 10–100s (0.01–0.1 Hz), microseismic band 1–10s (0.1–1.0 Hz) and short

period 0.1–1s (1.0–10 Hz). PSD results were compared to the high-noise and low-noise model of Peterson (1993), expressed in dB referred to  $1 \text{ (m/s}^2\text{)}^2\text{/Hz}$ . All 24 hours recorded data were used in the calculations, and no earthquakes data were included. The PSDs of noise were computed for each component at each station by extracting 10800 sec for broadband period processing during one complete year of continuous recording of seismic noise data. The data acquisition system records three orthogonal components (Vertical, North, and East). The response curves and the calibration sheets of seismometers were taken into consideration during processing steps.

All prospective data windows were visually inspected to ensure that obvious signals from local microearthquakes or other obvious cultural contaminants (e.g., mining explosions) were excluded. The power spectra are estimated by time averaging over modified periodograms (Welch 1967) in MATLAB. Each segment was divided into eight sections with 50 % overlap and then Fourier transformed.

To properly compare the estimated PSD calculation with the United States Geological Survey (USGS) noise models, the data sets have been run through the Peterson algorithm used to calculate the USGS noise models (Peterson 1993) and

compared PSDs. Generally, it is revealed that the algorithms produced the same PSDs at the same frequencies.

## RESULTS

The PSDs for all broadband stations have been calculated from at least 3 hours data windows during 1 year of continuous recording in 2009, 2010 and 2011 (Fig. 4). The three components are shown individually with Peterson's (1993) low- and high-noise models. The figures display the broadband period background noise PSDs over the entire experiment time at the following stations: AVE, IFR, ALHU, M001, NKM, M004, TAF, M012, M013, M015, M017, M018, M202, M206, M208, M210, M215, M218, MM07, MM08, MM10 and MM14. However, the mean or median of PSDs was not performed for each station, to distinguish between season's PSD variability and to construct upper and lower noise models.

The results reveal a large amount of variability in the PSD levels at all stations. The greatest variability can be observed at long periods in most stations. The dynamic range of our data extends from -180 dB ( $T > 40$  sec, vertical components) to -100 dB ( $f > 10$  Hz), covering about 80 dB of power. The least amount of variation can be observed in the 0.01–1.0 Hz frequency range, which corresponds to the microseismic frequencies. However, for  $T > 3$  sec, most PSDs for the vertical component lie on within a 15 dB interval. At short periods ( $T < 1$  sec) the difference in noise levels is higher, reaching 40 dB.

The horizontal components are much noisier at this period range, probably due to tilting effects associated with the physical installation settings (Bormann 2002), which do not perform as well as those used for permanent stations. The power of those components ranges between -125 and -155 dB for periods close to 20 sec and increases up to -120/ -150 dB at period close to 90 sec.

## DISCUSSION

Comparing the overall PSD levels of each component at each station with the USGS high- and low-noise models (Peterson 1993); namely, at high frequencies, the noise levels at all stations fell within the bounds of the noise models, with all components at similar PSD levels in the frequency band 1.0 to 50.0 Hz. Despite of the good vault design, the choice of quiet sites, and the adequate thermal insulation, the cultural effects contribute mostly to the variability at the higher frequencies. The sites most isolated from such activity show up well in short-period ranges and the PSDs fell within the bounds of the noise models for all components and are closer to the low-noise model (NLNM) than high-noise model (NHNM). Tilt, pressure, and wind are sources of noise for long period data, which easily increase the noise of the horizontal components in broadband data.

The observation of the seasonal and diurnal variations (Fig. 5) can distinguish several types of noise. The difference

between cultural noise and natural noise can be discriminated by observing day and night patterns (Peterson, 1993). Indeed, the observation of seasonal pattern can be isolated apart from the natural noise (microseisms, diurnal temperature and other atmospheric conditions). The long-period noise sources from temperature, tilt and pressure make horizontal components noisier than the vertical components.

This study could help to review the difference in noise level during annual sessions and determine the time required before the noise stabilizes after deployment. This information is useful for making decisions about the stability of the site in relation to several site locations. The PSDs for the horizontal and vertical component of each station after deployment were plotted at periods of 0.1, 1, 100, 873 s from available data.

## CONCLUSION

Results from noise analysis are useful for characterizing the performance of the recently deployed broadband stations for detecting operational problems. They should be relevant for choosing future locations of Scientific Institute backbone stations in the study area and optimizing the distribution of local network stations. We have presented a study on the seismic background noise spectra for the permanent and temporary seismographic networks in Morocco and identified the major sources of seismic noise in different frequency bands:

- At high frequencies the origin of the seismic background noise is clearly related to cultural sources and results in significant diurnal differences in the noise level.

- The microseismic band is related to the variations in the seismic noise between calm and stormy days as well as seasonal variations, with higher noise levels in the winter and the lowest levels in the summer.

- At long periods, the background noise level variations can be explained by the amplitude variations of infragravity waves arising from changes in the ocean wave intensities. In this frequency range, we have also detected diurnal variations of the seismic noise that can be associated with convective air movements around the sensor.

This work has enabled the detection of operational problems, leading to relocation of some stations and modifications in the sensor insulation techniques. It also studied the variations related to daytime, season, weather, location and the type of installation. In summary, the most likely prospect, for improving significantly the broadband noise environment in shallow portable broadband deployments below about 0.1 Hz, lies in a more detailed understanding of the local long-period noise environment. This is especially notable for horizontal components, where key details include improved understanding of how slab tilting effects are related to thermal, atmospheric pressure and ground effects interacting with vault design and near-surface site geology. This study could be considered as a first step towards the development of new seismic noise models in North Africa that was not included in Peterson (1993).

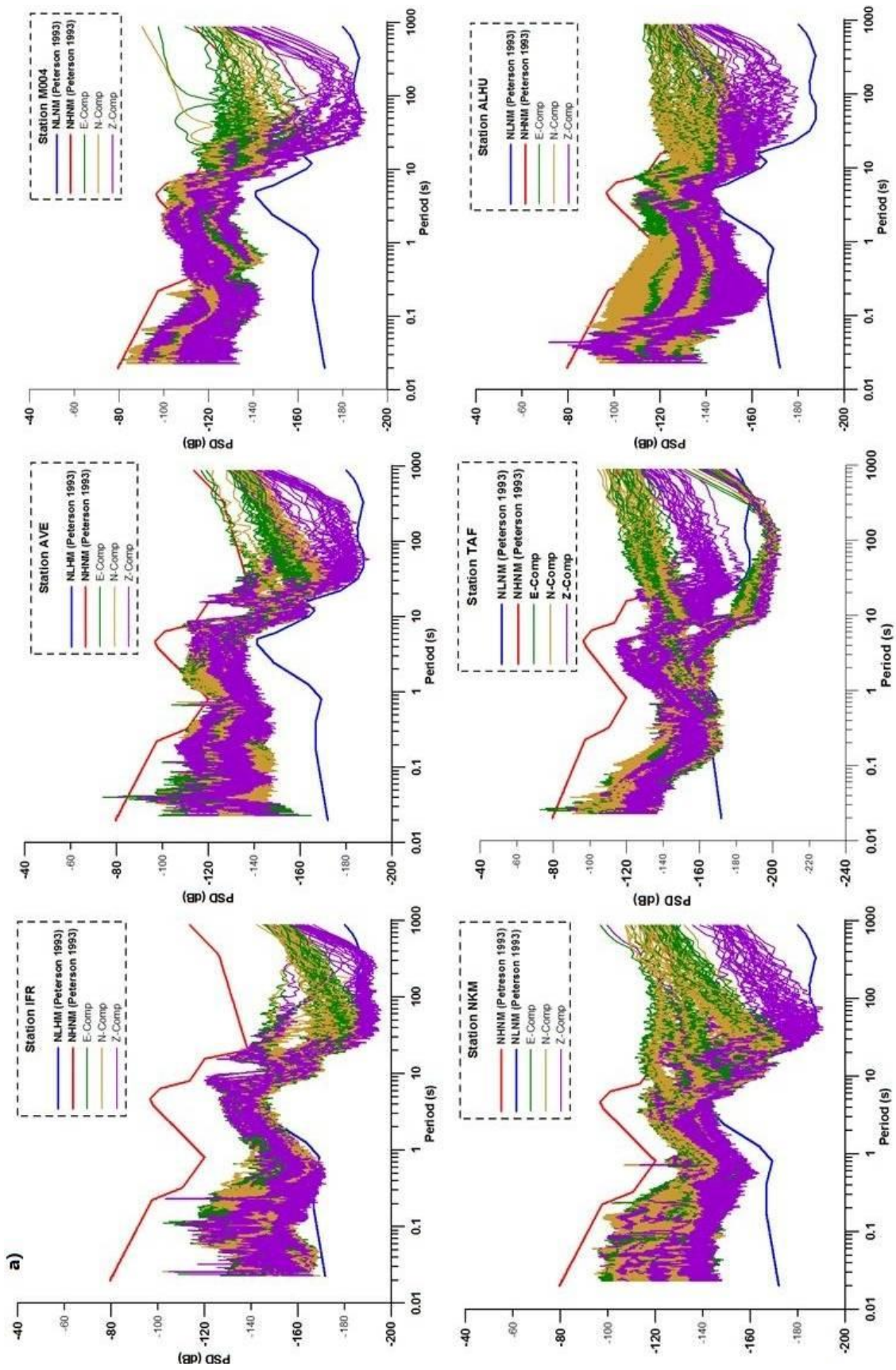


Figure 4. Power spectral density curves computed for the portable and permanent broadband seismic stations belonging to the studied networks. The curves corresponding to the Z, E and N components are drawn in violet, brown and green, respectively. The Peterson curves are represented in blue and red for comparison. a. Seismic stations: IFR, AVE, M004, NKM, TAF and ALHU.

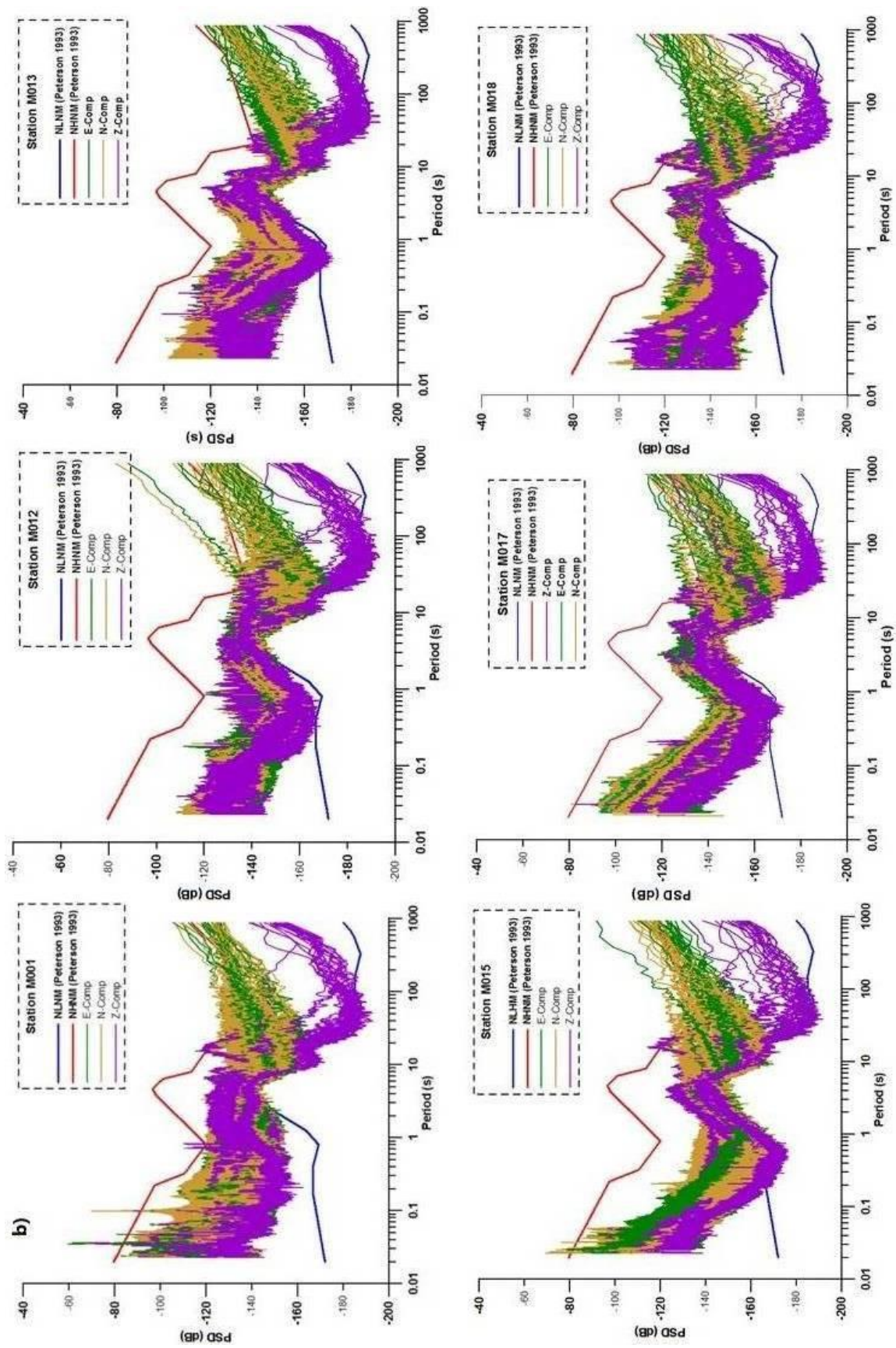


Figure 4. (continued 1). b. Seismic stations: M001, M012, M013, M015, M017 and M018.

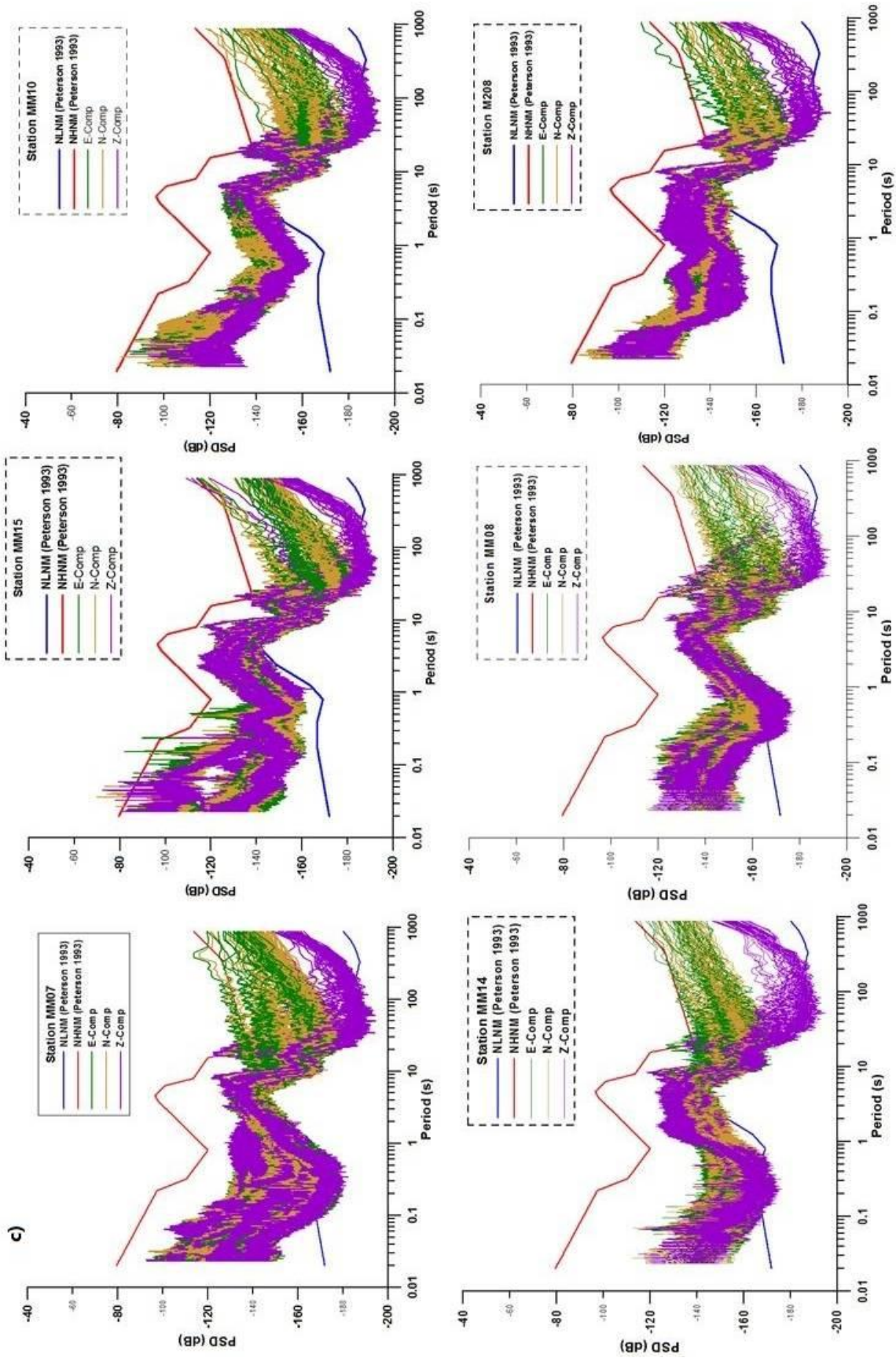


Figure 4. (continued 2). c. Seismic stations: MM07, MM08, MM10, MM14, MM15 and M208.

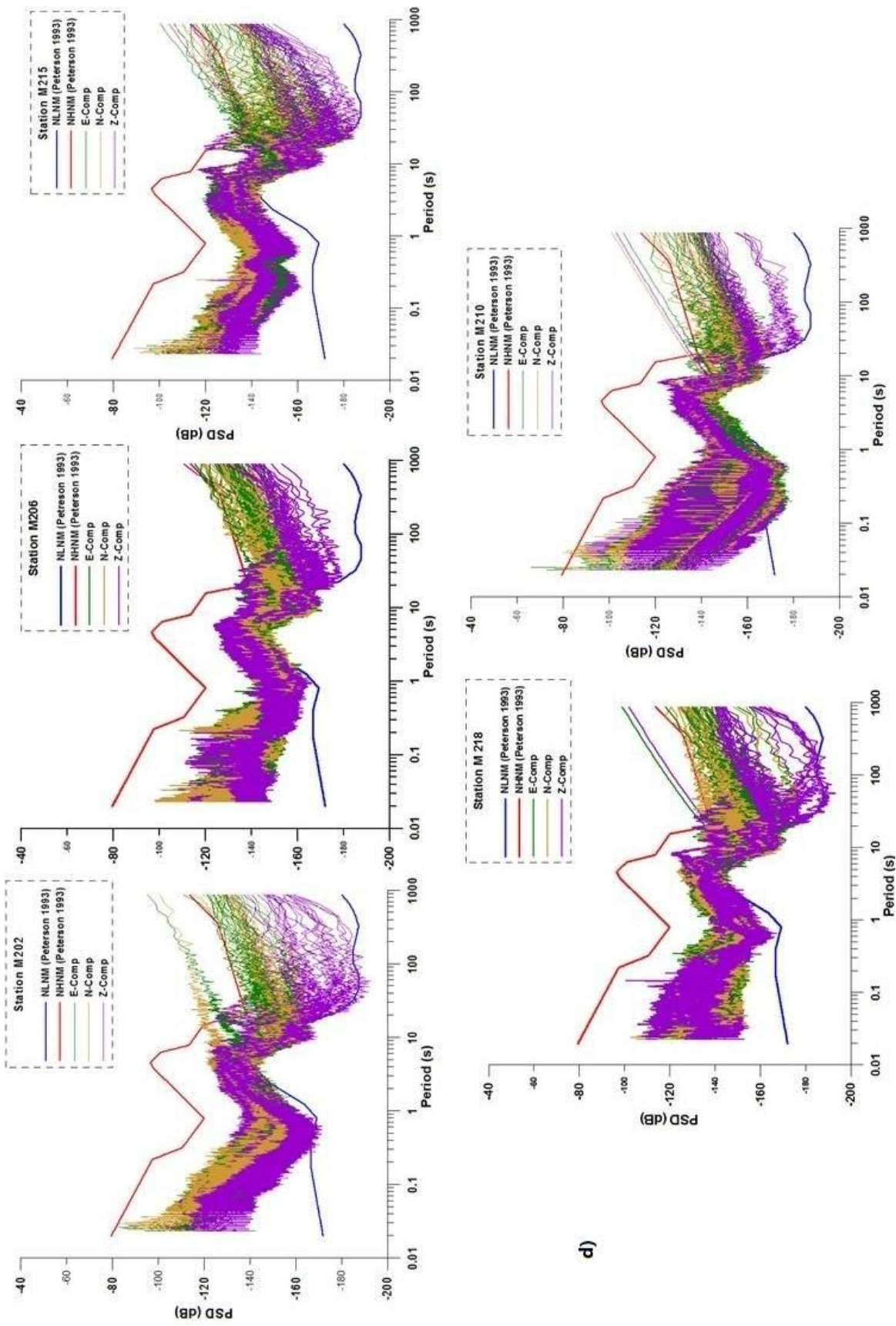


Figure 4. (continued 3). d. Seismic stations: M202, M206, M215, M218 and M210.

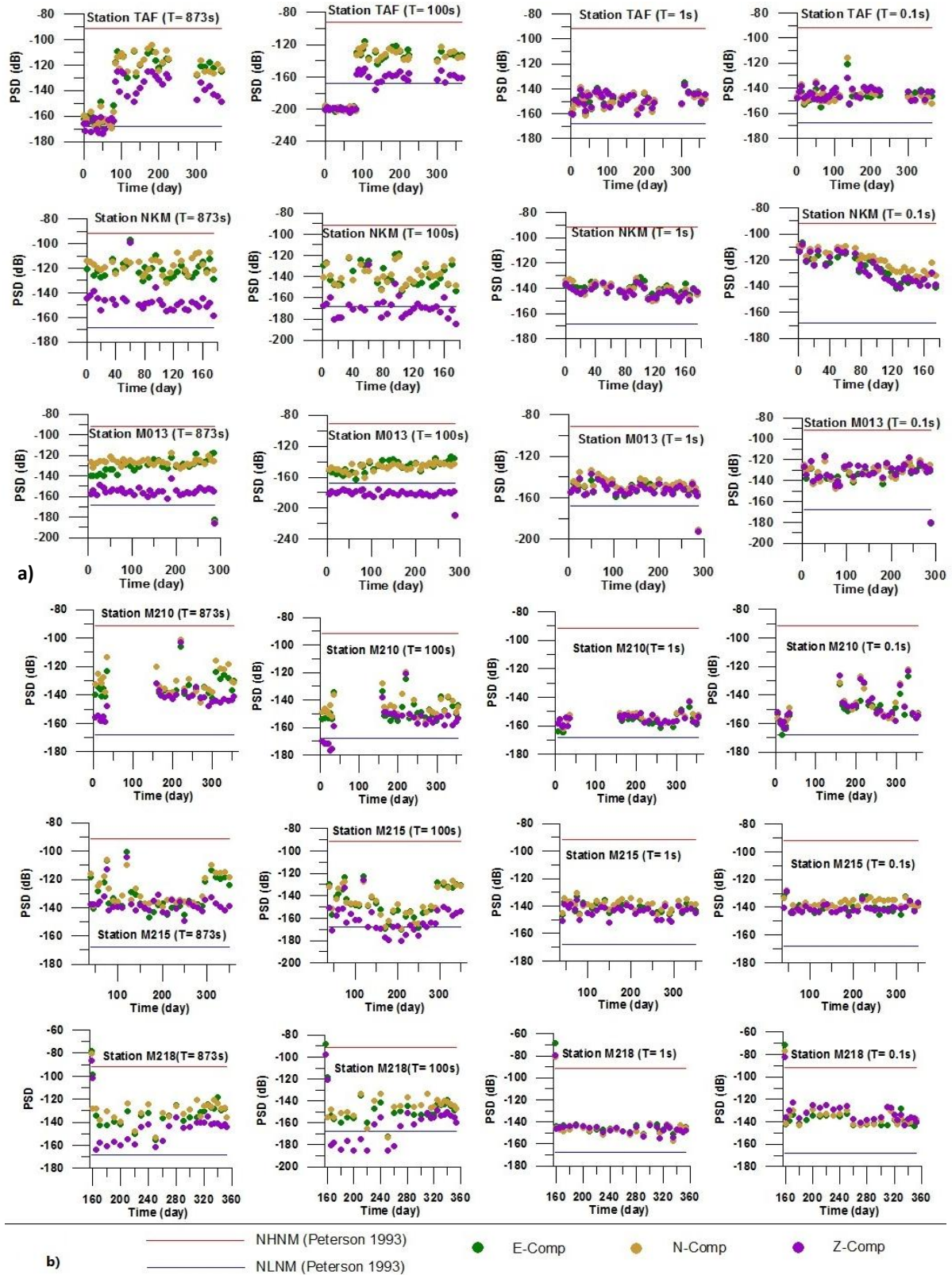


Figure 5. Seasonal variability of PSDs versus time for periods of 0.1, 1, 100 and 873 s, computed for the portable and permanent broadband seismic stations that make up the arrays. PSD values obtained from the Z, E and N components of the ground motion are plotted in violet, brown, and green, respectively. The USGS low-and high-noise levels are plotted in blue and red for comparison. a. TAF, NKM and M013 stations; b. M210, M215 and M218 stations.

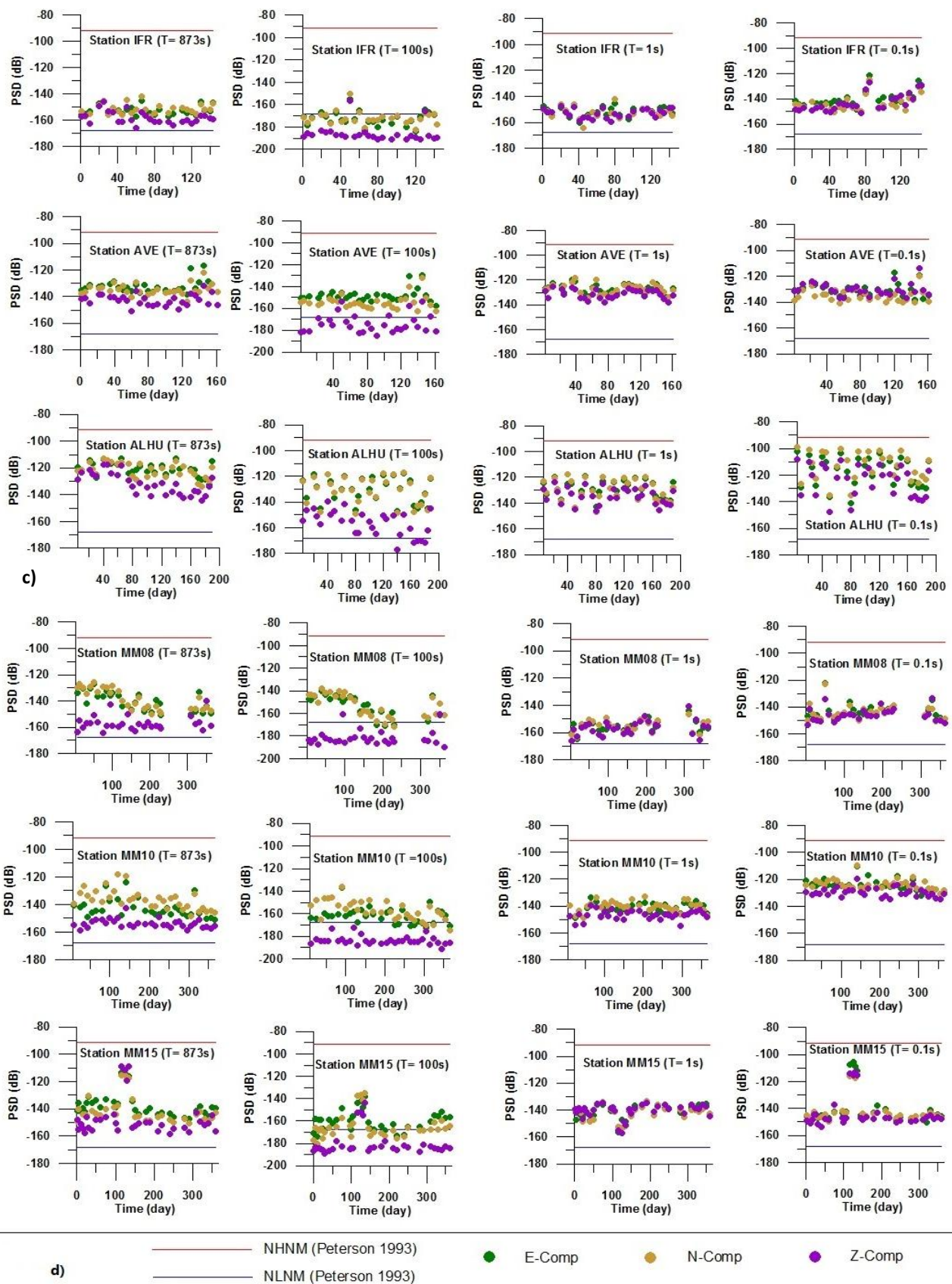


Figure 5. (continued 1). c. IFR; AVE and ALHU stations; d. MM08, MM10 and MM15 stations.

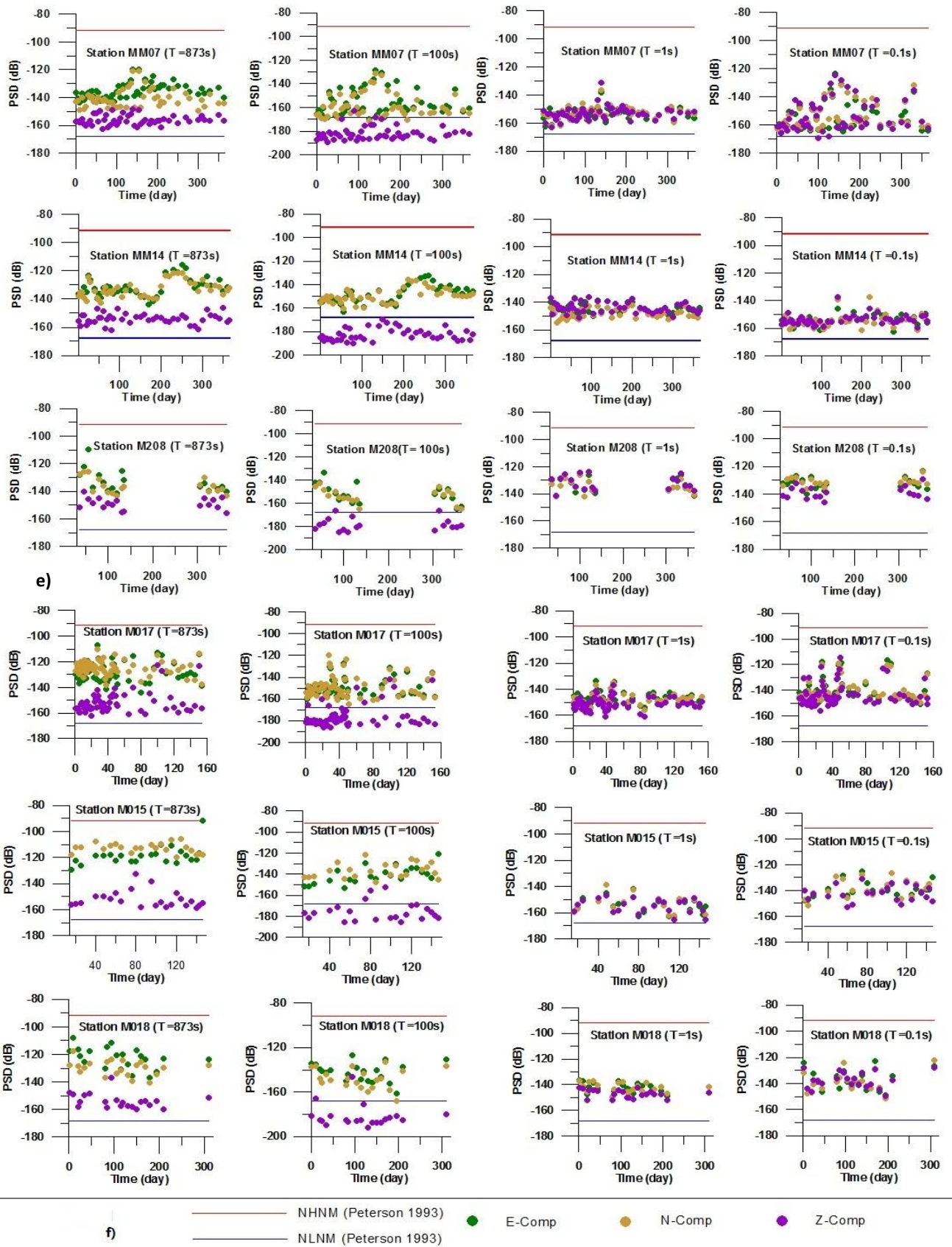


Figure 5. (continued 2). e. MM07, MM14 and M208 stations; f. M017, M015 and M018 stations.

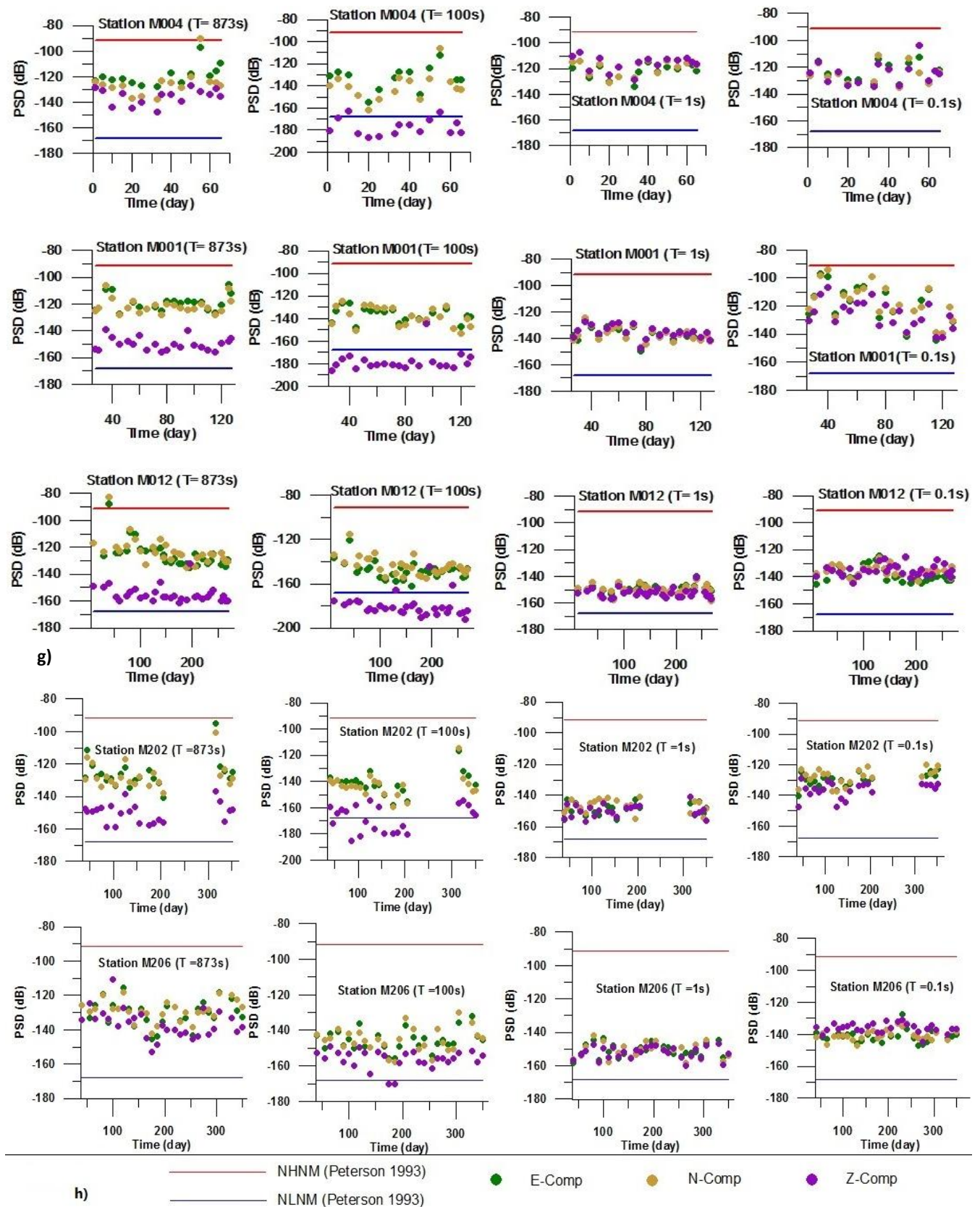


Figure 5. (continued 3). g. M004; M001; and M012 stations. H. M202 and M206 stations.

## ACKNOWLEDGMENTS

This study was sponsored by the Scientific Institute of the University Mohammed V, Rabat (Morocco). We strongly thank dozens of private landowners for their kind cooperation. We are also grateful to the Institute Jaume Almera, CSIC, Barcelona (Spain) and Institut für Geophysik, University of Münster (Germany) for their assistance during the installation of the stations. We also thank Professor José Badal for his comments and recommendations that led to a great improvement of this manuscript.

## REFERENCES

- Abd el-aal A.K. 2010a. Eliminating upper harmonic noise in vibroseis data via numerical simulation. *Geophysical Journal International*, 181, 1499–1509.
- Abd el-aal A.K. 2010b. Modeling of seismic hazard at the northeastern part of greater Cairo metropolitan area, Egypt. *Journal of Geophysics and Engineering*, 7, 75–90.
- Abd el-aal A.K. 2010c. Ground motion prediction from nearest seismogenic zones in and around Greater Cairo area. *Natural Hazards and Earth System Sciences*, 10, 1495–1511.
- Abd el-aal A.K. 2011. Harmonic by harmonic removal technique for improving vibroseis data quality. *Geophysical Prospecting*, 59, 279–294.
- Abd el-aal A.K. 2012. Very broadband seismic background noise analysis of permanent good vaulted seismic stations. *Journal of Seismology*, 17, 2, 223–237.
- Abd el-aal A.K. & Soliman M.S. 2013. New Seismic Noise Models Obtained Using Very Broadband Stations. *Pure and Applied Geophysics*, 170, 11, 1849–1857.
- Badal J., Chen Y., Chourak M. & Stankiewicz J. 2013. S-wave velocity images of the Dead Sea Basin provided by ambient seismic noise. *Journal of Asian Earth Sciences*, 75, 26–35.
- Bahavar M. & North R. 2002. Estimation of background noise for international monitoring system seismic stations. *Pure and Applied Geophysics*, 159, 911–944.
- Beauchamp W., Allmendinger R., Barazangi M., *et al.* 1999. Inversion tectonics and the evolution of the High Atlas Mountains, Morocco, based on a geological-geophysical transect. *Tectonics*, 18, 163–184.
- Beauduin P., Lognonne P., Montagner J., *et al.* 1996: The effects of atmospheric pressure changes on seismic signals, or how to improve the quality of a station. *Bulletin of the Seismological Society of America*, 86, 1760–1799.
- Berger J., P. Davis & G. Ekstrom. 2004. Ambient earth noise: a survey of the global seismographic network. *Journal of Geophysical Research*, 109, B11, 307. doi:10.1029/2004JB003408.
- Bormann P. (Ed.) 2002. *New Manual of Seismological Observatory Practice*. GeoForschungsZentrum Potsdam, Potsdam, Germany, Chapter 7, p. 15.
- Chouet B., De Luca G., Milana G. *et al.* 1998. Shallow velocity structure of Stromboli Volcano, Italy, derived from small-aperture array measurements of strombolian tremor. *Bulletin of the Seismological Society of America*, 88, 3, 653–666.
- D'Alessandro A., Badal J., D'Anna G. *et al.* 2013. Location performance and detection threshold of the Spanish National Seismic Network. *Pure and Applied Geophysics*, 170, 1859–1880.
- Diaz J., Villaseñor A., Morales J. *et al.* & Topolberia Seismic Working Group 2010. Background noise characteristics at the IberArray Broadband Seismic Network. *Bulletin of the Seismological Society of America*, 100, 2, 618–628.
- Dong-Hoon Sheen, Jin Soo Shin, Tae-Seob Kang, Chang-Eob Baag 2009. Low frequency cultural noise. *Geophysical Research Letters*, 36, L17, 314. doi: 10.1029/2009GL039625.
- Frizon de Lamotte D., Saint Bezar B., Bracène R. & Mercier E. 2000. The two main steps of the Atlas building and geodynamics of the western Mediterranean. *Tectonics*, 19, 4, 740–761.
- Galindo-Zaldívar J., Jabaloy A., Serrano I. *et al.* 1999. Recent and present-day stresses in the Granada Basin (Betic Cordilleras): Example of a late Miocene-present-day extensional basin in a convergent plate boundary. *Tectonics*, 18, 4, 686–702.
- Given H.K. 1990. Variations in broadband seismic noise at IRIS/IDA stations in the USSR with implications for event detection. *Bulletin of the Seismological Society of America*, 80, 2072–2088.
- Given H.K. & Fels F. 1993. Site characteristics and ambient ground noise at IRIS IDA stations AAK (Ala-Archa, Kyrgyzstan) and LY (Talaya, Russia). *Bulletin of the Seismological Society of America*, 83, 945–953.
- Gurrola H., Minster J.B., Given H. *et al.* 1990. Analysis of high frequency seismic noise in the western United States and eastern Kazakhstan. *Bulletin of the Seismological Society of America*, 80, 951–970.
- Laville E., Piqué A., Amrhar M. & Charroud M. 2004: A restatement of the Mesozoic Atlasic Rifting (Morocco). *Journal of African Earth Sciences*, 38, 2, 145–153.
- López-Casado C, Henares J., Badal J. & Peláez J.A. 2014. Multifractal images of the seismicity in the Ibero-Maghrebian region (westernmost boundary between the Eurasian and African plates). *Tectonophysics*, 627, 82–97.
- McNamara, D. E. & Buland R.P. 2004. Ambient Noise Levels in the Continental United States. *Bulletin of the Seismological Society of America*, 94, 4, 1517–1527.
- Medina F. & Cherkaoui T.E. 1988. Précisions sur le mécanisme au foyer du séisme d'Agadir (Maroc) du 29 Février 1960. Place dans le cadre sismotectonique du Maroc. *Geophysica*, 24, 57–66.
- Negredo A.M., Bird P., Sanz de Galdeano C. & Buforn E. Neotectonic modeling of the Ibero-Maghrebian region. *Journal of Geophysical Research*, 10, B11, 10-1–10-15. Peterson, J. 1993. *Observations and modelling of seismic background noise*. U.S. Geological Survey, open-file report, 93–322.
- Piqué A. & Michard A. 1989. Moroccan hercynides: a synopsis. The Paleozoic sedimentary and tectonic evolution at the northern margin of West Africa. *American Journal of Science*, 289, 286–330.
- Rodgers P.W., Taylo, S.R. & Nakanishi K.K. 1987. System and site noise in the regional seismic test network from 0.1 to 20 Hz. *Bulletin of the Seismological Society of America*, 77, 663–678.
- Sanz de Galdeano C. 1990. Geologic evolution of the Betic Cordilleras in the Western Mediterranean, Miocene to the present. *Tectonophysics*, 172, 107–119.
- Sleeman R., van Wettum A. & Trampert J. 2006: Three-channel correlation analysis: a new technique to measure instrumental noise of digitizers and seismic sensors. *Bulletin of the Seismological Society of America*, 96, 1, 258–271.

- Stankiewicz J., Weber M.H., Mohsen A. & Hofstetter R. 2012. Dead Sea Basin imaged by ambient seismic noise tomography. *Pure and Applied Geophysics*, 169, 615–623.
- Tahayt A., Mourabit T., Rigo A. et al. 2008. Mouvements actuels des blocs tectoniques dans l'arc Bético-Rifain à partir des mesures GPS entre 1999 et 2005. *Comptes Rendus Geoscience*, 340, 6, 400–413.
- Uhrhammer R.A., Karavas W. & Romanowicz B. 1998. Broadband seismic station installation guidelines. *Seismological Research Letters*, 69, 15–26.
- Uhrhammer, R.A. 2000. *Background noise PSD analysis of USNSN broadband data for 1998*. Berkeley Seismological Laboratory report, 22 p.
- Webb S.C. 1998. Broadband seismology and noise under the ocean. *Reviews of Geophysics*, 36, 1, 105–142.
- Welch P. 1967. The use of fast Fourier transform for the estimation of power spectra: a method based on time averaging over short, modified periodograms, *IEEE Trans. Audio Electroacoustics*, AU15, 70–73.
- Vila J. 1998. The broadband seismic station CAD (Tunel del Cadi, eastern Pyrenees): site characteristics and background noise. *Bulletin of the Seismological Society of America*, 88, 297–303.
- Wessel P. & Smith W., 1991. Free software helps display data, *EOS*, 72, 445–446.
- Withers M.M., Aster R.C., Young C.J. & Chael E.P. 1996. High frequency analysis of seismic background noise as a function of wind speed and shallow depth. *Bulletin of the Seismological Society of America*, 86, 1507–1515.
- Young C.J., Chael E.P., Withers M.M., Aster R.C. 1996. A comparison of high frequency (>1 Hz) surface and subsurface noise environment at three sites in the United States. *Bulletin of the Seismological Society of America*, 86, 1516–1528.
- Zhang J., Gerstoft P. & Shearer P.M. 2009. High frequency P-wave seismic noise driven by ocean winds, *Geophysical Research Letters*, 36, 9, L09, 302. doi:10.1029/2009/GL037761.
- Zhang H-J., Zhou H., Abd el-aal A.K. & Zhang J. 2012. The anti-correlation method for removing harmonic distortion in vibroseis slip-sweep data. *Applied Geophysics*, 9, 2, 159–167.
- Zürn W. & Widmer R. 1995. On noise reduction in vertical seismic records below 2 mHz using local barometric pressure. *Geophysical Research Letters* 22, 24, 3537–3540.

Manuscrit reçu le 24/04/2014  
Version révisée acceptée le 28/11/2014  
Version finale reçue le 14/06/2015  
Mise en ligne le 23/06/2015